Int. J. Multiphase Flow, Vol. 3, pp. 415–443. Pergamon/Elsevier, 1977. Printed in Great Britain

METHODS AND CORRELATIONS FOR THE PREDICTION OF QUENCHING RATES ON HOT SURFACES

S. K. W. Yu, P. R. Farmer and M. W. E. Coney
Central Electricity Research Laboratories, Kelvin Avenue, Leatherhead, Surrey, U.K.

(*Received* 25 *July* 1976)

Abstract—A substantial quantity of experimental data on rewetting, much of which has not been previously reported, is analysed using the results of calculations of the two-dimensional conduction processes taking place in the walls of tubes, which have been used to simulate the cladding of nuclear fuel elements. Correlations giving the quenching heat-transfer coefficient and sputtering temperature are proposed as a result of the analysis. These correlations may be combined with the previously reported conduction analysis to predict rewetting rates under a wide range of conditions.

The new data include falling film rewetting rates measured for a range of system pressures (1–15 bars), initial wall temperatures (200–650°C), coolant mass flowrates (3–50 g sec^{-1}) and subcoolings (0–90°C). Measurements have also been made of rewetting rates by bottom flooding of both saturated and subcooled water at atmospheric pressure.

1. INTRODUCTION

A considerable number of papers have now been published on the subject of rewetting hot surfaces—and a review of those concerned with basic studies produced by Butterworth & Owen (1975). It is generally accepted that experimental data can be reasonably well described by means of a theoretical model which assumes that the quench front velocity is determined by the rate at which heat can be conducted from the hot dry surface through the metal to the wetted area where it is removed by boiling. The physical mechanisms controlling the boiling heat-transfer coefficient h and the temperature at which the surface first wets (the so-called sputtering temperature T_0) are not understood, and controversy exists as to the most suitable form to take for these parameters. With regard to the conduction process it is fairly clear that a two-dimensional model offers the best description, though under some circumstances this may be simplified to a one-dimensional approximation.

The present paper follows on from an earlier publication by Coney (1974) in which the solution of the two-dimensional conduction equation for the heat flow in the metal was expressed analytically in terms of two infinite series expansions. The calculation of accurate numerical results involved taking a considerable number of terms in these expansions (up to 151 were used) and necessitated a computer program being written. In his treatment Coney assumed that the heat-transfer coefficient h between the metal surface and the water in the wetted region (i.e. where the wall temperature is less than T_0) was a constant. The calculations were performed for the case of a plane surface and it was assumed that they can be applied to a cylindrical tube by defining an equivalent plane surface thickness as the metal cross-sectional area divided by the wetted perimeter. The same assumption is made here also. The predictions of the theory were applied by Coney (1974) to experimental rewetting data obtained by Bennett *et al.* (1966) and the values for the heat-transfer coefficient h and the sputtering temperature T_0 were deduced. However the experimental data analysed were only a small fraction of the available data on rewetting.

The observation of nucleate boiling behind the quench front has led to the suggestion, put into practice by Thompson (1972) that a power law variation of heat-transfer coefficient should be applied. However, Thompson's argument that experimental evidence supported his statement was shown by Coney (1974) to be invalid. It will be seen here that the experimental data may be interpreted using the assumption of a constant heat-transfer coefficient (which incidentally does not vary with the initial wall temperature) and in any case it is clear that present

ignorance of the heat-transfer mechanisms in the very narrow, high heat-flux zone ($\sim 10^8$ W m^{-2}) of the quench front means that the choice of a more complex representation for the heat-transfer coefficient cannot be justified. For example, it is doubtful if nucleate boiling persists right up to the quench boundary and it is possible that conduction and surface evaporation in an extremely thin liquid film (~ 1 μm), (probably subject to rapid oscillations of the boundary as surface irregularities are overcome), is the more important mechanism determining the variation of the heat-transfer coefficient (see Wayner *et al.*, 1976). A further point of consideration is that even if nucleate boiling does persist up to the quench boundary, the behaviour of the heat-transfer coefficient near the critical heat flux is very different from the power law behaviour at low superheat temperatures.

The present paper describes the systematic analysis of all the data on falling film rewetting which were known to the authors at the time when the analysis was performed, and which contains sufficient information for the analysis to be carried out. For this purpose a further computer program was developed which calculates best fit values of heat-transfer coefficient and sputtering temperature using the two-dimensional conduction theory. This paper also describes the results of our own measurements of falling film rewetting rates at pressures between atmospheric and 15 bars, including the effects of water flowrate and inlet subcooling. Previous experimental data are combined with these data to produce correlations for h and T_0, which enable falling film rewetting rates to be predicted over a wide range of conditions.

In addition, bottom flooding experiments have been performed at atmospheric pressure. It will be seen that the bottom flooding correlations are consistent with the falling-film correlation for saturated flows, but that there are substantial differences where the water at the quench front is subcooled. Limited bottom flooding data from other authors have been examined but no attempt has been made to carry out an exhaustive survey as was done with the falling film data.

None of this work has been previously reported in the open literature although some data analysis work and the bottom flooding experiments have been reported in rather more detail than given here at private meetings of the European Two-Phase Flow Group.

The high pressure falling film experiments have only been reported in an internal C.E.G.B. document.

2. APPLICATION OF THE THEORY TO EXPERIMENTAL DATA

2.1 *Computed results of the rewetting theory*

The model, which is illustrated in figure 1, is basically similar to that used by previous authors (e.g. Yamanouchi 1968). In the quenching region (which can be regarded as extending an overall distance of about ten times the wall thickness) it is assumed that no heat is lost or gained by the cladding except in the wetted region upstream of the quench front where the heat-transfer coefficient is h (W m^{-2} °C^{-1}). The cladding, which is initially at temperature T_w (°C) cools by conduction until the surface reaches T_0 (°C), at which point it wets. The temperature of the water in the region of the quench front is T_q (°C). Outside the quenching region the model permits all the normal heat-transfer mechanisms to be taken into account. In the pre-quench region these mechanisms determine the wall temperature T_w prior to rewetting, while in the post-quench region the various heat-transfer mechanisms determine the quench front water temperature T_q and of course the final wall temperature after the whole process is complete. If the inlet water temperature T_i (°C) is at or near saturation, or if there is ample heat-transfer to the water film, the quench water temperature T_q will reach the saturation temperature T_s.

The mathematical solution of the conduction problem in the region of the quench front has been fully described by Coney (1974) and only such details as are necessary to understand its application to the experimental data will be given here. The calculation was carried out using a computer program (REWET) and expressed in terms of three non-dimensional parameters which describe the conduction process. These parameters are defined below. The dimensionless

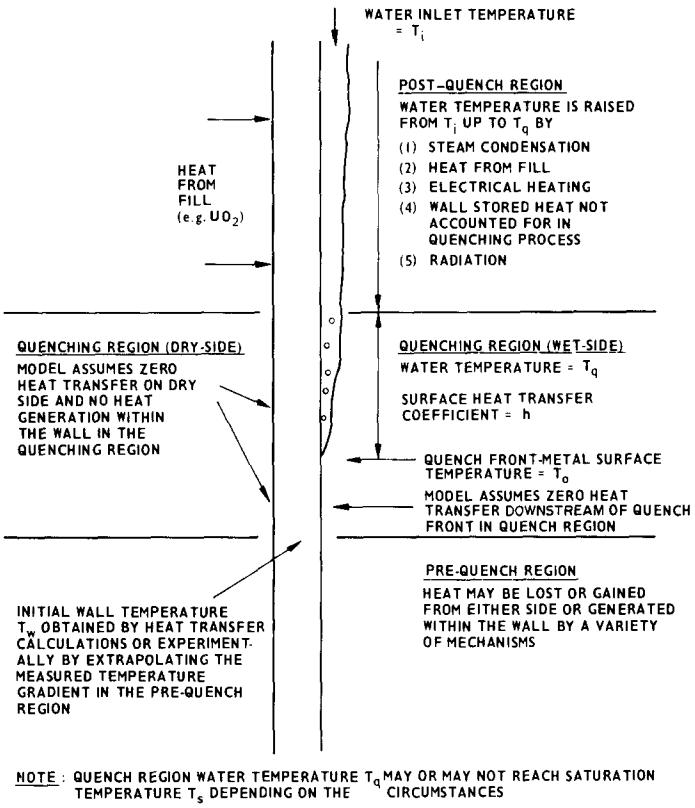

Figure 1. Illustration of the rewetting model (shown for the falling film case, but also applicable by inversion of the diagram to bottom flooding).

inverse wetting rate w is defined by

$$w = \frac{k}{\rho c \epsilon U} \qquad [1]$$

where U (m sec^{-1}) is the velocity of the quench front and k, ρ, c and ϵ are respectively the thermal conductivity (W m^{-1} °C^{-1}), density (kg m^{-3}), specific heat (J kg^{-1} °C^{-1}) and thickness (m) of the cladding. The dimensionless initial wall temperature ψ is given by

$$\psi = \frac{T_w - T_q}{T_0 - T_q} \qquad [2]$$

and the heat-transfer coefficient is expressed in terms of the Biot Number Bi, where

$$Bi = \frac{h\epsilon}{k}. \qquad [3]$$

The program REWET was used to calculate values of ψ for values of Bi between 0.1 and 200 and of w from zero up to values sufficiently large for the variation of ψ with w to become linear. The results were shown graphically by Coney (1974).

The calculations showed that for a wide range of practical interest (i.e. $Bi \geq 5$), the value of w was largely determined by the value of the quantity $\psi/\sqrt{(Bi)}$. Since this observation has important implications for the analysis of the data it is convenient to define a further

dimensionless parameter η by the equation

$$\eta = \frac{\psi}{\sqrt{(Bi)}}. \quad [4]$$

Furthermore if we define a function F_q, $(W\,°C)^{1/2}\,m^{-1}$, by the equation

$$F_q = (T_0 - T_q)\sqrt{h}, \quad [5]$$

it follows that

$$\eta = \frac{(T_w - T_q)}{F_q}\sqrt{\left(\frac{k}{\epsilon}\right)}. \quad [6]$$

If the water at the quench front is saturated, T_q becomes T_s and F_q becomes F_s.

After some consideration, the authors decided that the most convenient form of table for the purposes of prediction of rewetting velocities in practical situations would be achieved by inverting the computed results and expressing w in terms of η and Bi as seen in table 1. Table 1 also shows the equations recommended by the authors for extrapolation outside the range of

Table 1. Values of w as a function of Bi and η $(=\psi/\sqrt{(Bi)})$

η	Bi	0.1	0.5	1	2	5	10	20	30	50	100	150	200	
0.1												.0027	.0041	←extrapolate→ using $w = K\left(\eta^2 - \frac{\eta}{\sqrt{Bi}}\right)$ where K is given in Table 2 (for $w \leq 0.25$)
0.2									.0053	.0166	.0263	.0300	.0318	
0.3			$w = 0$					.0329	.0482	.0618	.0732	.0777	.0799	
0.4			when $\eta = \frac{1}{\sqrt{Bi}}$				.0488	.0948	.112	.127	.141	.146	.1480	
0.5						.0400	.127	.177	.198	.213	.227	.231	.235	
0.6			(in practice rewetting is no longer conduction controlled when $\eta \leq \frac{1}{\sqrt{Bi}}$)			.131	.225	.275	.294	.310	.324	.328	.330	extrapolate→ by assuming no change in the values of w with increasing Bi
0.7						.243	.331	.380	.397	.412	.425	.429	.431	
0.8					.114	.359	.440	.486	.501	.517	.529	.533	.536	
0.9					.250	.473	.548	.590	.606	.621	.633	.637	.639	
1.0				0.00	.387	.593	.654	.695	.710	.723	.736	.739	.740	
1.2				.337	.634	.802	.864	.903	.914	.928	.941	.942	.943	
1.5			.199	.751	.970	1.115	1.172	1.212	1.219	1.233	1.244	1.245	1.246	
2			.989	1.320	1.499	1.627	1.679	1.713	1.723	1.734	1.746	1.746	1.746	
3			2.112	2.411	2.522	2.635	2.681	2.718	2.728	2.738	2.746	2.746	2.746	
4	extrapolate ↓ by taking the lower of the values given by (1) $w = 1.57\left(\eta^2 - \frac{\eta}{\sqrt{Bi}}\right)$ and (2) $w = \sqrt{\eta^2 - \frac{\eta}{\sqrt{Bi}}}$	1.776	3.154	3.385	3.531	3.640	3.683	extrapolate + using $w = \eta - C_2$ where C_2 varies as follows				extrapolate ↓→ using $w = \eta - 0.254$		
5		2.991	4.175	4.396	4.541	4.641	4.683							
7		5.152	6.197	6.407	6.542	6.643	6.684							
10		8.242	9.211	9.415	9.547	9.644	9.685							
15		13.30	14.22	14.42	14.55	14.64	14.69							
		extrapolate + using $w = \left(\eta^2 - \frac{\eta}{\sqrt{Bi}}\right)^{\frac{1}{2}} - C_1$ where C_1 varies as follows						.282	.272	.262	.254			
		.03	.05	.07	.09	.13	.16							

the table. Further information on these equations (expressed in terms of ψ rather than η) may be obtained from Coney (1974). Figure 2 illustrates graphically the variation of w with η and Bi.

Table 2 shows the variation of the coefficient K used in the equation

$$w = K\left(\eta^2 - \frac{\eta}{\sqrt{(Bi)}}\right). \qquad [7]$$

This equation may be used over the full range of Biot Numbers, provided the value w predicted by it is less than about 0.25.

On the accuracy of the data given in tables 1 and 2 it should be noted that the computer calculations are not exact and depend upon a sufficient number of terms being taken in two series expansions. For this reason the accuracy of the last figure of each tabulated number cannot be relied upon. Again some further details are available from Coney (1974).

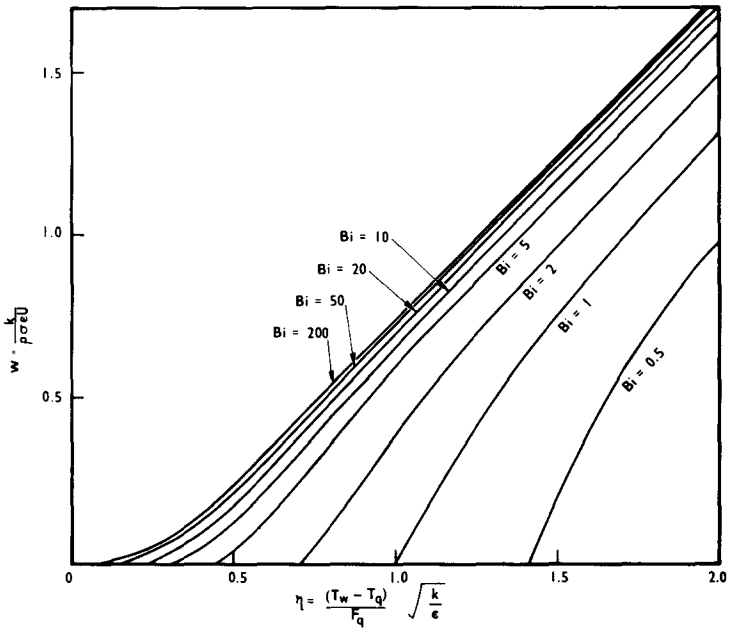

Figure 2. Variation of the non-dimensional inverse wetting rate w with η and the Biot number Bi.

Table 2. Variation of the coefficient K with $\eta\sqrt{(Bi)}$

$\eta\sqrt{(Bi)}$	1.0	1.2	1.5	2.0	2.5	3.0	4.0	5.0	6.0	7.0
K	1.570	1.478	1.395	1.315	1.256	1.220	1.172	1.139	1.117	1.094

2.2 *Material properties used in the calculations*

For the purposes of the calculations described here the material properties were assumed to be linear functions of temperature. For the calculation of the dimensionless inverse wetting rate w, the material properties were evaluated for each data point at a temperature mid-way between the initial wall temperature T_w and the quench water temperature T_q. For the calculation of the heat-transfer coefficient from the Biot Number, the properties were evaluated at the sputtering temperature T_0. Table 3 shows the equations used, where T is in °C.

Property evaluations actually required for the data analysed in this paper all lie within the temperature range of 66°C up to 418°C for stainless steel and inconel and within the range 191°C to 467°C in the case of zircaloy. The relevant tables indicate which properties were used with each set of data. Uncertainties in the property data and inaccuracies in the linear ap-

Table 3. Material properties used in the calculations

Property set	Material	Thermal conductivity (W m^{-1} °C^{-1})	Density (kg m^{-3})	Specific heat (J kg^{-1} °C^{-1})
1	Stainless steel	$14.7+0.0136T$	$7980-0.4T$	$477+0.188T$
2	Stainless steel	$14.65+0.0161T$	$7980-0.4T$	$461+0.21T$
3	Inconel	$14.0+0.0168T$	$8420-0.363T$	$488+0.218T$
4	Zircaloy	$10.0+0.016T$	$6573-0.0763T$	$285+0.1T$

proximations will obviously cause some degree of error in the calculation. In the case of stainless steel there are small variations in the properties according to the type of steel used, which is not always specified by the authors concerned. We note that to a rough approximation

$$F_q \sim \rho c \sqrt{\left(\frac{\epsilon}{k}\right)} U(T_w - T_q),$$

thus F_q is least sensitive to those properties (k and ϵ) which are subject to the greatest uncertainty, while ρ and c are less likely to be in error. While the effects of uncertainties or errors in the property data are not negligible (amounting to about ±5% in F_q for the temperature ranges given above) they are considerably less than the experimental scatter in U and $(T_w - T_q)$.

2.3 *Method of application of the theory*

In order to make predictions of rewetting rates it is necessary to know the initial clad temperature, the material properties, the functional dependence of the various dimensionless groups and the actual values of the heat-transfer coefficient h and sputtering temperature T_0. At present h and T_0 can only be obtained empirically by analysing rewetting experiments to obtain a two-parameter fit to the data.

The method of approach used is to assume that h and T_0 are constants for a given set of data points. A set of data is one in which T_w is the only independent variable and U is the dependent variable. All other parameters such as pressure, flowrate, inlet subcooling and of course the test section itself remain unchanged within a given set of data. Corresponding values of w can be readily calculated from the measured values of U and the material properties. Appropriate values of T_q, the quench water temperature are calculated by the method described in the Appendix. A range of values of Bi is then applied together with the theoretical relationships of Tables 1 and 2 to calculate a table of values $(T_0)_{ij}$ of the sputtering temperature, where i denotes the data point and j the assumed value of Bi. Thus for each Bi chosen, an average sputtering temperature for all the data points in that set can be obtained

$$(T_0 - T_q)_{\text{av}} = \frac{1}{N} \sum_{i=1}^{N} \frac{(T_w - T_q)}{\eta_{ij} \sqrt{(Bi_j)}} \qquad [8]$$

where N is the number of data points.

The deviation of the experimentally measured wall temperatures from the values implied by the average value of $(T_0 - T_q)$ is expressed by the r.m.s. deviation σ_j (°C) where

$$\sigma_j^2 = \frac{1}{N} \sum_{i=1}^{N} \{(T_w - T_q)_i - \eta_{ij} \sqrt{(Bi_j)} (T_0 - T_q)_{\text{av},j}\}^2. \qquad [9]$$

The best fit value of Bi is then chosen by interpolation as the value which gives the lowest value of σ, which we than call σ_{MIN}.†

The large number of data points available for analysis, the fairly large scatter in the data, and the relative insensitivity of σ_j to Bi_j (associated with the appropriate average value of $T_0 - T_q$) in the range of interest necessitated the writing of a computer program. This program contains an inverted form of Table 1 giving values of ψ (rather than η) in terms of w and Bi, and an interpolation routine to obtain intermediate values. Graphical output routines are incorporated to provide a visual display of the measure of agreement between theory and experiment.

3. THE EXPERIMENTAL RIGS

3.1 *The high pressure falling film rig*

A schematic diagram of the test facility is shown in figure 3. The rig consists of a stainless steel loop and a mild steel pressure vessel. Demineralized water is taken from the bottom of the pressure vessel by a gear pump, passed through coolers and a flowmeter, and returned to the vessel, where it is either sprayed onto the heated test section or diverted back to the bottom of the vessel. The rig is pressurized by boiling the water in the vessel. The coolers, needle control valves and two 3 kW trim heaters are arranged so that the spray flow rate and its subcooling can be closely controlled. In addition the pipework inside the vessel carrying the spray water to the test section can be trace heated by a proportion of the circulating flow being passed through an outer jacket.

The spray flow is measured by a thermal flowmeter capable of covering a range of flows from 2 to 50 g sec^{-1}. Assuming negligible heat losses, the flow rate can be calculated from the heat balance between the electrical input to the heater and the heat carried away by the water. To minimize the effect of heat loss a heated jacket is fitted round the outside of the flowmeter and the whole assembly lagged. The amount of heat supplied to the jacket is controlled to maintain equal temperatures between the flowmeter and the jacket. The flowmeter was calibrated by comparing the calculated flow from the heat balance with that measured directly by weighing. It was found that the calculated flow was within ±2% of the measured value for flows higher than 25 g sec^{-1}, and to within ±5% for flows between 2 and 25 g sec^{-1}.

The pressure in the main vessel is maintained by a pressure controller adjusting the power input to a 60 kW immersion heater. The rig was designed for a maximum operating pressure of 40 bar, but owing to an insurance limitation on the heater, it was only operated up to 15 bar for the series of tests described in this paper. Future work will cover higher pressures.

The tubular test section is heated electrically by an a.c. power supply and the inside pressurized with nitrogen to prevent it collapsing when heated at high rig pressures. Tube wall temperatures were measured using two rings of glass fibre insulated chromel–alumel thermocouples welded to the inside surface of the test section. The rings (each of which contained eight thermocouples) were spaced 8 cm apart, and the first ring was 7 cm below the two jets used to spray the water on to the test section. The thermocouple outputs were fed to a u.v. recorder. The diameter of the spray jets could be varied in the range 2–7 mm to keep the jet velocity between 40 and 80 cm sec^{-1}. This was found to help maintain an even water film on the test section surface. Test section data and the range of operating conditions covered are given in table 4.

†As one of the referees has pointed out, there are other possible ways of performing the two-parameter fit. For instance it would be possible to perform the averaging (c.f. [8]) on F_q for fixed values of T_0 and then perform the standard deviation analysis (not necessarily on $T_w - T_q$) to determine the best value of T_0. Alternatively a two-stage standard deviation analysis could be performed by first optimising F_q for fixed values of T_0 and secondly choosing the best combination of F_q and T_0. On the basis of the computer plots (eq. figures 6, 7, 9 and 10) which were obtained in all cases, the authors think it is unlikely that significant improvements in the fit could be obtained using these alternative methods and any alterations to the derived correlations would be very minor.

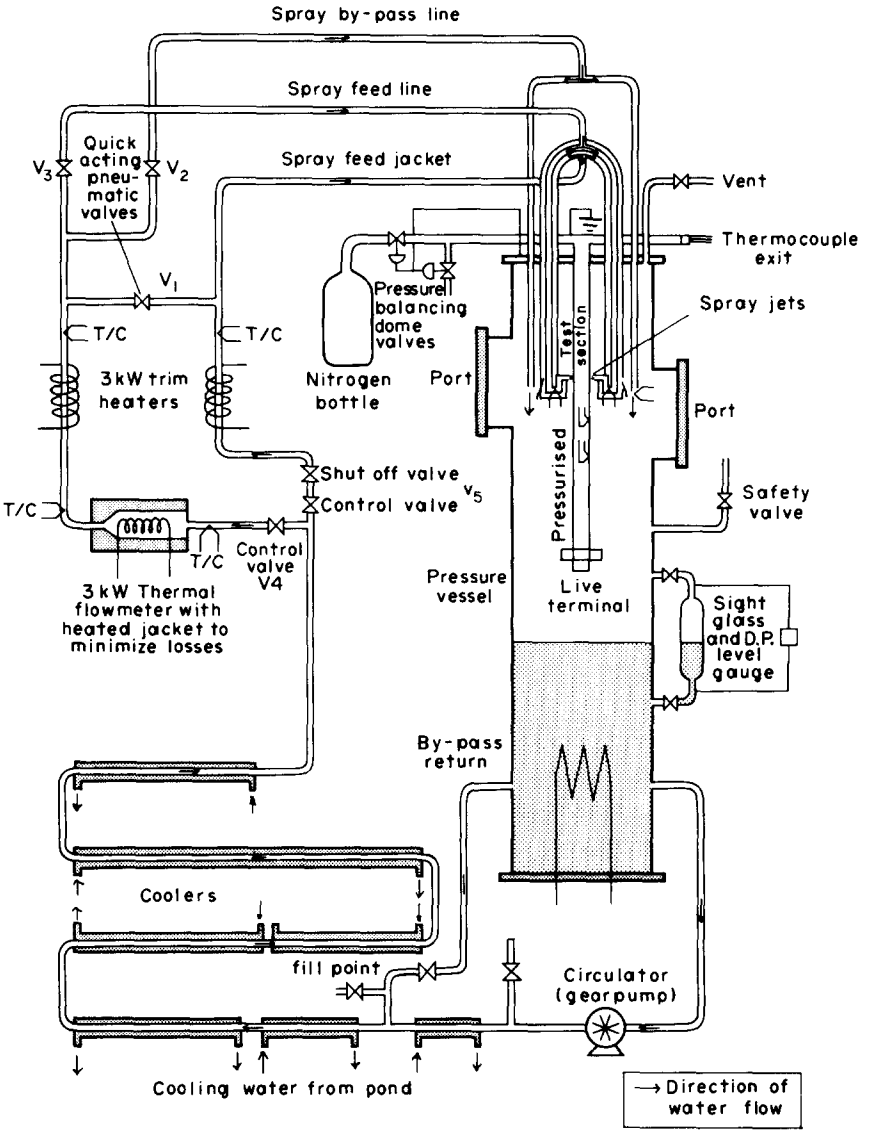

Figure 3. Flow diagram of the high pressure falling film rig.

3.2 *The atmospheric bottom flooding rig*

The requirement was for a test facility that was the simplest extension of the falling film equipment into bottom flooding geometry. Thus it was decided to use initially the same test section tubing and cool it on the inside—this enabled thermocouples to be attached very easily by spot welding them to the outside of the tube. Subsequently a second tube was used with a thicker wall.

A schematic diagram of the apparatus is shown in figure 4. Water is taken from a header tank, drawn through a flexible impeller pump, thence to one of two variable area flowmeters and into a heating section. From the heating section the flow path divides to go either up the test section and back to the header tank, or through a parallel by-pass section. Operation of a single valve diverts the flow from one path to the other. For test purposes the test section was initially heated in the dry state (again using low voltage a.c.) with the circulating water going through the by-pass. The diverter valve was then operated to flood the test section. Test section temperatures were measured using 20 thermocouples. Near the tube centre there were two rings of four thermocouples spaced 3 cm apart. The remainder were spaced in line axially at an average separation of 8 cm.

Table 4. Range of parameters used in the experiments

Test section	Initial dry wall temperatures (°C)	Coolant flowrate (g sec^{-1})	Coolant subcooling (°C)	System pressure (bar)
Falling film experiments Type 321 Stainless steel O.D. 15.9 mm Wall 0.71 mm Length 830 mm	200–650	3–50	0–90	1–14.8
Bottom flooding experiments Type 321 Stainless steel A. { O.D. 15 mm, Wall 0.71 mm	300–800	A. 1–200	0–70	Atmospheric only
B. { O.D. 16.3 mm, Wall 1.8 mm		B. 2–150		
Length 1 m approx.				

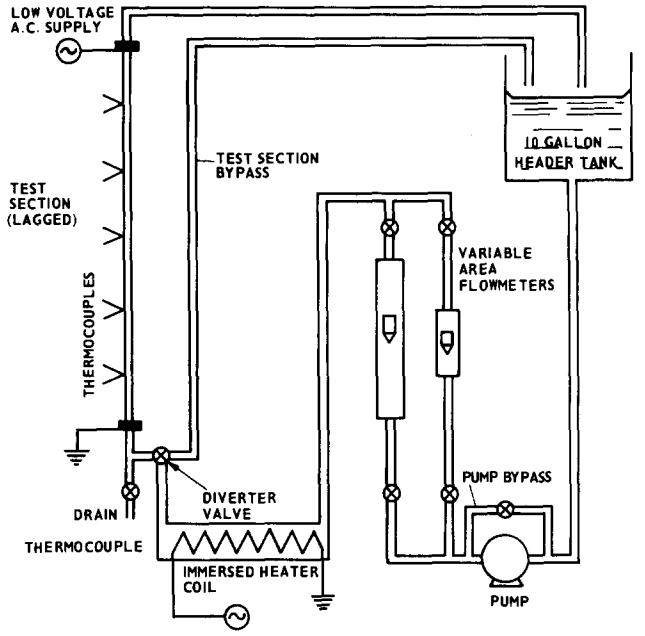

Figure 4. Schematic diagram of the atmospheric bottom flooding rig.

4. EXPERIMENTAL RESULTS

Figure 5 illustrates a typical u.v. plot from the falling film rig showing one upstream and one downstream thermocouple. From such records the rewetting velocities and mean wall temperatures at the quench fronts were obtained. As the front passes each thermocouple there is a rapid fall in temperature from the initial dry wall value to near saturation. Determination of the actual moment of quenching is not possible, but all that is necessary is that a reproducible point is selected. The method chosen was to take the intersection of the gradients of the trace before the arrival of the front, and at the steepest part of the transient. The technique is illustrated on figure 5. These intersections gave the moment of quenching and the tube wall temperature (T_w) at that time. The co-ordinates of these points were produced on punched cards using a pencil follower. The quench front velocity was calculated from the elapsed time between the quenching of the first thermocouple on the top ring of eight and the first on the lower ring. The

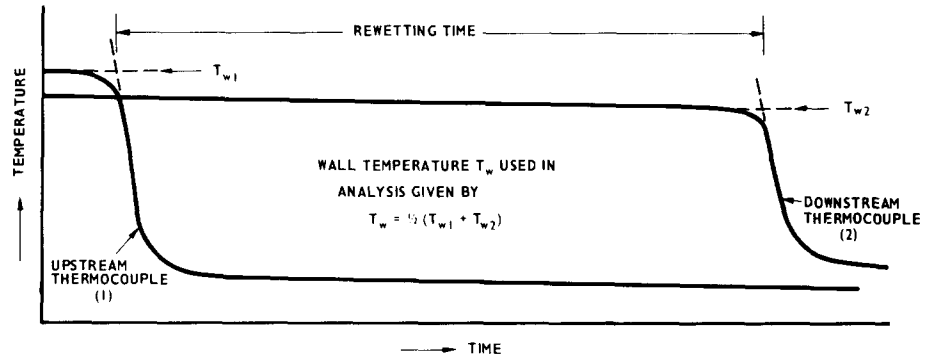

Figure 5. Illustration of typical temperature traces and the method of obtaining wall temperature T_w and the rewetting time.

mean wall temperature T_w was calculated as the arithmetic mean of the two individual wall temperatures.

The same methods were used to obtain T_w and U for the bottom flooding experiments, though the rate of fall of tube temperature in advance of the quench front was much higher because of the considerably increased pre-quench heat-transfer.

4.1 *Falling film experiments with saturated water*

All these tests were performed in a steam environment and the water temperature at the jets was very close to saturation (less than 3°C subcooling). Table 5 shows the various conditions investigated giving the range of wall temperatures examined and the number of data points obtained in each case. The results of the analysis described in Section 2.3 are given for each case in terms of the best fit values of Bi, $T_0 - T_s$, F_s and the minimum standard deviation σ_{MIN}. Figures 6 and 7 show two examples of the results of the fitting process compared to the experimental data.

Table 5 shows that for most data sets σ_{MIN} is about 10°C or less indicating a close fit to the data. For some data sets (e.g. 3 g sec^{-1} at 1 bar pressure) the program was unable to obtain a minimum for σ by varying Bi. Usually the fit continued to improve slightly as Bi was increased up to the maximum allowed by the program. Taking the above example a change in Bi from 100 to 999 only reduced σ from 11 to 10.2°C which shows the relative insensitivity of the accuracy of the fit to the value of the Biot Number (if the appropriate sputtering temperature for that Biot Number is chosen). This behaviour is entirely consistent with the insensitivity to the value of Bi shown in Table 1. In view of this, values for $Bi > 999$ are not considered realistic because of the enormous values of h they imply and so the fit for $Bi = 999$ was taken as the nearest. Figure 6 shows that the final curve fits the points quite well.

Two observations were made during the course of the experiments.

(a) During the early runs rewetting rates showed progressive increase with time but subsequently remained constant. Other authors (Piggott & Porthouse 1975) have noted this and the effect was thought to be due to initial surface oxidation.

(b) Leaving the electrical power on or turning it off during a run did not affect the result. This agrees with theoretical calculations by Thompson (1972), and experimental data by Bennett *et al.* (1966).

4.2 *Falling film experiments with subcooled water*

Similar conditions of flow and wall temperature to those used for the saturated water tests were employed, but only three pressures (1, 3.43 and 7.87 bar) were examined, and a range of subcoolings up to 90°C was covered. The results are given in table 6, where ΔT_q is defined as equal to the difference between T_s and T_q.

Table 5. The best fit Biot number, $(T_0 - T_s)$ and F_s obtained for the CERL falling film rig using saturated water

Pressure (bar)	Flow (g sec^{-1})	Range of T_w (°C)	No. of data points	Biot number (Bi)	$T_0 - T_s$	σ_{MIN} (°C)	F_s $\times 10^{-4}$
1.01	3	190–500	10	999*	8.0	10.2	3.83
(atmos.	5	248–526	7	8.6	76.3	8.3	3.51
pressure)	7	201–566	12	999*	8.5	10.8	4.17
	10	207–504	7	11.9	62.1	48.1	3.33
	15	253–600	9	5.0	116.1	10.0	4.16
	15	236–592	9	5.0	120.8	19.2	4.42
	15	230–401	8	65.0	36.0	4.0	4.47
	20	216–567	12	29.6	52.9	7.9	4.47
	30	209–564	8	20.8	59.6	4.3	4.23
	40	216–570	9	20.8	65.7	4.6	4.68
	40	218–577	11	118.0	29.0	7.0	4.83
	40	411–653	4	8.0	89.3	13.0	3.99
2.05	3	229–551	9	397.9	14.3	4.1	4.39
	15	269–511	11	32.6	49.7	7.8	4.44
	22.5	266–572	11	34.2	49.6	5.2	4.54
	30	269–591	11	30.2	53.7	4.9	4.63
3.43	3	217–361	5	49.6	43.4	4.8	4.81
	7.5	228–432	9	42.6	47.2	4.0	4.85
	15.0	279–589	11	27.8	62.9	5.3	5.26
	22.5	266–579	11	338.0	17.5	5.0	5.00
	30	225–570	9	30.8	57.5	9.3	5.05
	30	325–576	9	11.6	94.4	3.3	5.17
7.87	3	315–415	6	14.4	94.7	12.9	5.99
	7.5	302–554	11	49.6	57.3	6.5	6.47
	15	276–560	11	26.6	91.8	10.6	7.71
	22.5	271–550	11	37.4	68.4	8.1	6.75
	30	346–572	4	82.0	42.9	9.7	6.19
	30	275–561	11	20.0	99.8	8.7	7.29
14.8	7.5	321–575	10	27.8	109.3	17.0	9.57
	15	353–542	8	18.0	148.8	18.0	10.63
	22.5	293–592	11	29.6	108.3	15.1	9.78
	30	335–561	10	16.4	147.1	20.9	10.05

*Denotes cases where no minimum σ was obtained.
Material data from property set 2 in Table 3.

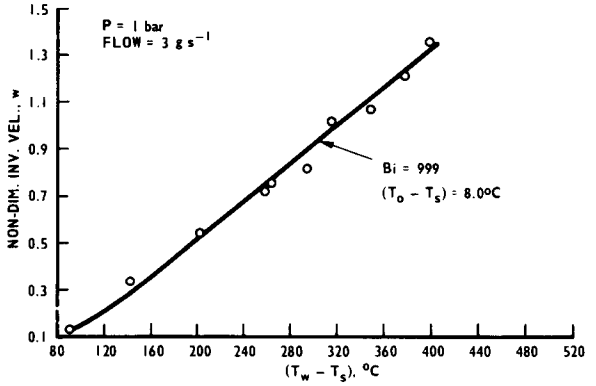

Figure 6. Comparison between the calculated curve and the spray cooling rig data at a pressure of 1 bar and a flow of 3 g sec^{-1}.

A number of experimental observations were made:

(a) For a given jet water temperature there was a strong effect of flow rate on rewetting rate.

(b) Increasing subcooling increased the rewetting rate (see figure 8).

(c) With high subcoolings the quench front tended to form rivulets down one side of the

Table 6. The best fit values of Bi, $(T_0 - T_q)$, F_q and α from the CERL falling film rig for a range of subcoolings and flow rates

Pressure (bar)	Flow (g sec^{-1})	ΔT_i (°C)	ΔT_q (°C)	T_w Range (°C)	No. of data points	Bi	$T_0 - T_q$	σ_{MIN} (°C)	$F_q \times 10^{-4}$	α
1.01	3	10	0	200–412	8	300*	15.0	5.5	4.03	1.11
	5	34	10	269–574	7	1.28	189.6	31.6	3.60	0.951
	5	34	10	230–572	9	314	16.8	14.9	4.61	1.22
	7	10	2	202–522	9	300*	15.0	9.0	4.02	1.04
	10	35	21	217–576	7	20.0	83.2	12.8	5.93	1.49
	10	35	21	262–568	8	18.0	92.7	17.3	6.30	1.58
	20	10	4	222–571	7	9.8	90.0	12.1	4.53	1.08
	20	30	22	225–566	8	38.4	60.1	9.5	5.87	1.40
	20	30	22	213–620	10	6.0	133.8	30.1	5.35	1.27
	20	60	47	326–581	7	300*	33.4	21.9	8.50	2.02
	20	60	47	217–620	12	39.8	93.7	13.9	9.36	2.22
	30	35	28.5	280–653	6	15.2	125.8	17.1	7.96	1.83
	30	65	55	294–577	7	53.8	114.4	3.5	13.36	3.08
	40	10	7.5	206–568	7	84.0	35.4	12.3	5.08	1.15
	40	37	30	212–604	8	300*	32.5	32.5	8.72	1.96
	40	80	70	294–680	7	500*	40.3	22.5	13.60	3.06
	50	65	58	284–639	4	27.8	138.1	14.8	11.44	2.53
3.43	30	10	7	227–549	9	384	18.8	34.6	5.84	1.02
	30	30	22	225–584	9	636	19.2	11.7	7.62	1.33
7.87	15	10	3	430–670	9	6.2	203.1	17.8	8.57	1.33
	15	30	18	476–624	5	94.0	62.1	18.6	9.82	1.52
	15	30	18	334–624	8	26.6	112.2	13.9	9.65	1.50
	22.5	10	7	321–573	11	18.4	118.3	10.3	8.53	1.32
	22.5	40	28	353–579	14	22.0	127.9	18.8	10.03	1.55
	22.5	40	28	315–579	8	13.4	154.3	9.9	9.55	1.47
	22.5	40	28	332–564	7	10.4	174.4	11.7	9.58	1.48
	40	10	7	325–588	9	9.5	165.8	8.3	8.75	1.34
	40	30	24	327–600	8	13.4	174.1	18.7	10.89	1.67
	40	60	49	374–583	7	5.52	278.7	46.3	11.54	1.77
	40	90	75	327–585	5	27.2	191.3	23.8	16.80	2.58

*Denotes cases where no minimum σ was obtained and Bi was chosen at the edge of the plateau in the curve of σ vs Bi. Material data from property set 2 in table 3.

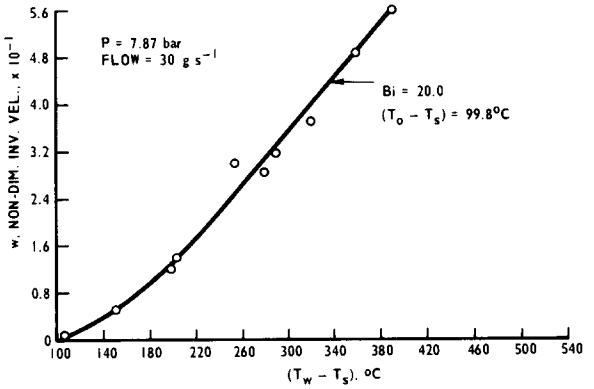

Figure 7. Comparison between the calculated curve and the spray cooling rig data at a pressure of 7.87 bar and flow of 30 g sec^{-1}.

test section rather than falling with uniform velocity. Quench data were always based on the leading edge of the rivulet when this happened.

Some correlations for rewetting rates using subcooled water have based the water temperature on that measured at the jet (e.g. Yoshioka & Hasegawa 1970; Piggott & Porthouse 1975). Clearly this cannot be correct since the water reaching the quench front could have received heat from four possible sources:

(a) Heat given up by any "fill" in the test section (e.g. the UO_2 fuel in a reactor), which does not take part in the quenching process.

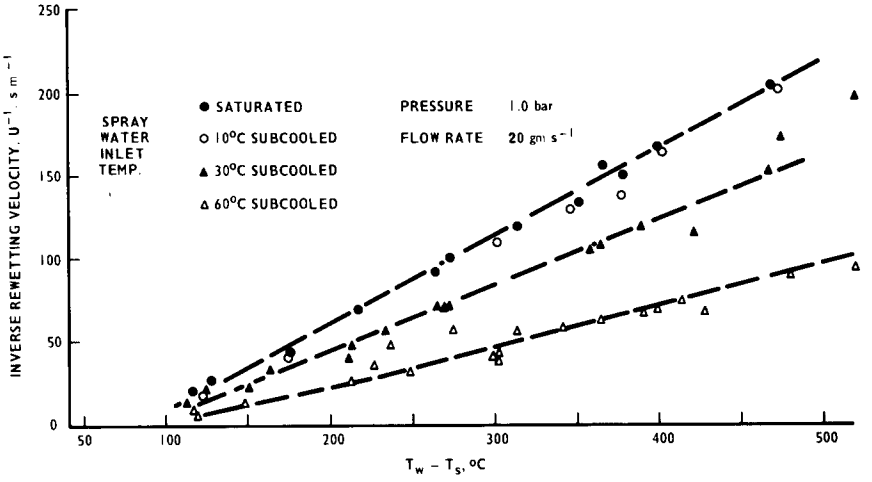

Figure 8. The effect of initial spray water temperature on the falling film rewetting rate.

(b) Electrical heating.

(c) Steam condensation into the falling water film.

(d) Heat stored in the clad not accounted for in the quenching process.

Obviously not all these sources apply to any one case, and in a reactor there may be other important mechanisms (e.g. radiation from adjacent rods). The appendix gives details of the methods of calculation which enable the water temperature at the quench front to be obtained. This temperature, T_q, was used in place of T_s when calculating the results given in table 6. There must inevitably be some uncertainty attached to the calculated figure of T_q and this is probably partly responsible for the generally higher values of σ_{MIN} obtained in the experiments with subcooled water.

4.3 *Bottom flooding experiments*

For any given values of coolant flowrate and temperature several experiments were performed using different initial dry wall temperatures as given in table 4. Despite this wide range of starting temperatures the values for T_w (the initial wall temperature at the moment of quenching) were limited to below about 650°C. This was because the pre-quench heat transfer process removed heat from the tube more quickly when it was at a higher temperature.

For almost all the runs the top thermocouples quenched out of sequence with those lower down, showing the presence of a falling film rewetting front initiated on the cold tubing near the top current clamp. In some cases this film extended well down the test section. No attempt was made to analyse the data from thermocouples quenched this way.

Tables 7 and 8 show the calculated values for Bi, F_s or F_q, $(T_0 - T_s)$ or $(T_0 - T_q)$, obtained from the curve fitting program. The data were analysed in exactly the same way as those from the falling film experiments—the assumption being made when calculating T_q that the water temperature was uniform across the tube.

Three observations can be made on the results:

(a) The Biot numbers obtained with saturated water are much lower than those obtained from the falling film studies—the range of values being 1–27 compared with 5–120. With subcooled flows in bottom flooding the Biot numbers are comparable with those from the falling film work.

(b) Over half the data sets from subcooled flows in test section A failed to allow best fit curves to be obtained. No reason for this was apparent from an examination of the raw data.

(c) The values of σ_{MIN} obtained were significantly higher than those obtained in the falling film experiments. It appeared that this was entirely due to scatter in the data rather than to any

Table 7. The best fit Biot number, $(T_0 - T_s)$ and F_s obtained for the two test-sections in bottom flooding rewetting for a range of flowrates with saturated water

Test-section	Flow (g sec^{-1})	Range of T_W (°C)	No. of points	Biot number	$T_0 - T_s$ (°C)	σ_{MIN} (°C)	$F_s \times 10^{-4}$
'A'	1	240–412	30	0.95	127.6	22.6	1.95
	2	250–452	25	5.04	85.3	19.5	2.94
	4	191–410	50	2.84	101.5	30.5	2.65
	7	219–356	27	0.98	124.8	16.6	1.93
	20	178–301	31	5.68	79.2	7.7	2.89
	30	240–290	15	6.16	80.6	9.6	3.07
	40	178–318	39	4.08	83.2	12.5	2.58
	100	209–304	22	4.24	120.4	20.0	3.88
	200	209–274	23	2.20	133.3	16.5	3.11
	20	184–416	56	10.1	74.6	25.0	3.63
	40	207–425	30	5.04	97.9	16.1	3.40
	12	200–426	28	26.6	52.3	15.3	4.08
'B'	2	231–511	24	1.34	160.2	48.6	1.90
	4	224–537	26	6.0	100.8	38.2	2.46
	12	215–446	31	11.9	79.9	14.9	2.72
	40	248–490	28	5.2	135.6	15.4	3.13
	8	195–440	56	11.9	72.8	29.1	2.47
	20	203–463	43	10.4	90.9	16.7	2.91
	92	247–375	20	3.28	159.2	47.0	2.95
	150	245–496	32	3.92	174.0	32.8	3.54

Material data from property set 2 in table 3.

Table 8. The best fit Biot number, $(T_0 - T_q)$ and F_q obtained for the two test-sections in bottom flooding rewetting for a range of flowrates and subcoolings

Test-section	Flow rate (g sec^{-1})	ΔT_i (°C)	ΔT_q (°C)	Range of T_w (°C)	No. of points	Bi	$(T_0 - T_q)$ (°C)	σ_{MIN} (°C)	$F_q \times 10^{-4}$	α
'A'	2	30	18	201–435	28	11.6	65.7	20.5	3.38	1.53
	2	70	58	167–360	30	200*	16.5	9.8	3.54	1.60
	4	30	24	187–425	23	290	14.7	23.8	3.68	1.50
	4	70	64	159–463	23	350	18.8	48.6	5.08	2.08
	8	30	27	216–470	30	92	38.7	27.8	5.50	2.03
	8	60	57	186–418	24	999*	13.8	32.1	6.62	2.44
	12	30	30	234–490	27	454	23.0	35.6	7.21	2.50
	20	30	30	201–440	29	999*	16.3	17.8	7.82	2.51
	20	60	60	216–550	27	999*	26.0	35.6	12.4	4.00
	40	60	60	158–555	29	999*	41.4	58.6	19.8	5.74
	40	70	70	210–600	24	999*	49.7	71.0	23.8	6.90
	100	30	30	213–595	26	999*	49.8	40.4	23.9	6.02
	100	70	70	281–600	25	266	135	50.1	39.2	9.89
'B'	100	70	70	360–643	43	132	244	55.7	28.8	7.00
	40	70	70	344–602	43	106	173	39.9	17.8	4.95
	20	70	70	333–620	42	49.6	178	35.3	12.5	3.87
	12	70	70	327–581	43	18.0	212	34.7	9.13	3.05
	8	70	67	310–564	42	13.1	219	40.8	8.08	2.86
	8	30	27	280–510	41	4.4	189	43.2	4.06	1.44
	12	30	30	293–545	39	70.6	78.2	21.0	6.39	2.13
	20	30	30	232–492	46	272	52.0	25.9	8.24	2.54
	40	30	30	248–508	48	25.4	191	47.3	9.85	2.74
	100	30	30	240–573	47	106	169	54.7	17.6	4.28
	100	15	15	240–507	47	29.6	163	43.7	9.03	2.19
	40	15	15	250–448	43	15.2	144	31.3	5.67	1.58
	20	15	15	193–397	53	17.6	110	24.9	4.58	1.41
	12	15	15	172–423	51	13.1	110	23.8	3.96	1.32
	8	15	12	218–438	54	10.1	113	20.7	3.58	1.27
	4	70	64	180–510	51	22.4	120	33.1	5.55	2.18
	2	70	58	200–473	43	116	122	35.3	4.09	1.78
	2	30	18	193–472	42	17.2	86.4	28.8	3.52	1.54
	4	30	24	223–492	50	6.8	142	37.0	3.73	1.47
	4	15	9	242–439	53	6.2	121	28.4	3.00	1.18
	2	15	3	228–537	45	2.52	152	51.0	2.46	1.07

*No minimum σ obtained.
Material data from property set 2 in table 3.

inability of the theory to represent the shape of the curve. Again the values of σ_{MIN} were higher in the subcooled experiments than in the saturated ones.

4.4 *Previous saturated and subcooled falling film experiments*

An extensive amount of data on rewetting by falling films was obtained by Elliott & Rose (1970, 1971) who measured rewetting rates on four different test-sections at various pressures (3.43–52.8 bar) and flow rates (7.5–30 g/sec). Rewetting took place on the inside of the tubular test-sections each of which consisted of a tube 965 mm long, 15.9 mm external diameter with a 1.27 mm thick wall. The wall temperatures used in the analysis described here were calculated using the simple average of the upstream and downstream thermocouple measurements, which required information additional to that given in the published reports (D. G. Elliott, A. D. Richards, private communication).

In the experiments of Bennett *et al.* (1966) rewetting took place on the outer surface of a stainless steel tube which had an outside diameter of 12.7 mm and a wall thickness of 1.63 mm. In this case pressures in the range 6.9–69 bar were investigated and there was some investigation of the effect of flowrate. However since no effect of the flowrate could be detected in either set of experiments the data for the various flowrates have been grouped together. The water at the quench front is believed to have been at saturation temperature in all the above experiments. Two comparisons between the fitted curves and experimental points are shown in figures 9 and 10.

Previous data on rewetting at atmospheric pressure with subcooled water have been obtained by Duffey & Porthouse (1972), Shires *et al.* (1964) and Yamanouchi (1968). Table 10

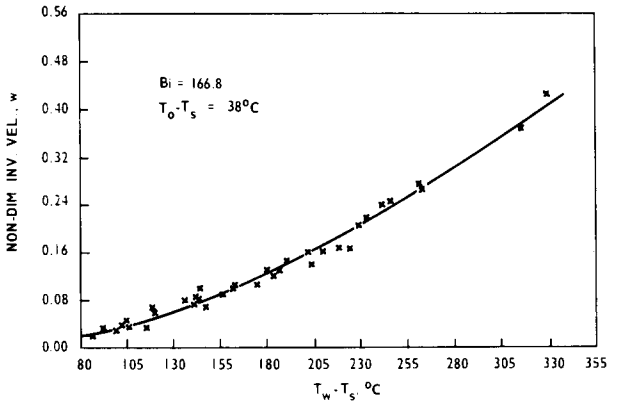

Figure 9. Comparison between the calculated curve and the Elliott & Rose (1970) first series stainless steel data at a pressure of 3.43 bar.

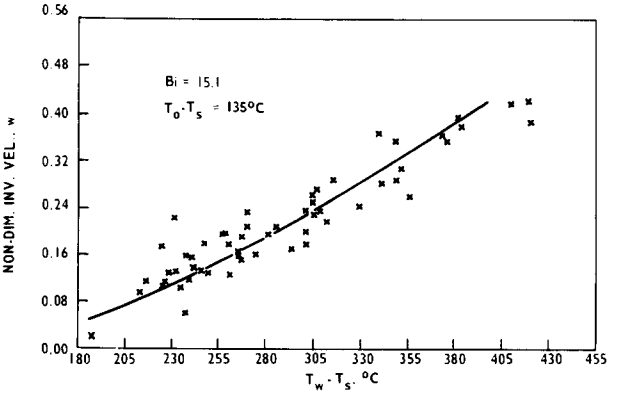

Fig. 10. Comparison between the calculated curve and the Elliott & Rose (1970) second series stainless steel data at a pressure of 3.43 bar.

shows the flows investigated and the subcooling at the quench front calculated by the methods of Appendix 1. Table 10 also shows the best fit Biot number, σ_{MIN}, $(T_0 - T_q)$ and F_q.

5. CORRELATION OF RESULTS

5.1 *Falling films with saturated water*

Having obtained values of $(T_0 - T_s)$ or $(T_0 - T_q)$ and F_s or F_q from a variety of different experiments it is necessary to analyse and correlate these results in order that predictive calculations may be performed. Probably the most important feature of Table 5–10 is that while F_s or F_q show reasonably consistent behaviour, the values of $(T_0 - T_s)$ or $(T_0 - T_q)$ and Bi show a wide variation. This arises from the theoretically derived results illustrated in figure 2 which show that provided $Bi \geq 5$ the rewetting velocity is very much determined by $(T_w - T_q)$, F_q and the material properties. The values of h and T_0 individually have very little effect.

This behaviour can also be demonstrated by plotting the quenching heat-transfer coefficient h vs $(T_0 - T_s)$ as shown in figure 11 for the case of the saturated falling-film data obtained by the present authors. It is seen that the experimental points at any given pressure lie close to lines having constant values of $(T_0 - T_s)\sqrt{h}$. This suggests a correlation of the form

$$(T_0 - T_s)\sqrt{h} = f(P). \qquad [10]$$

Until recently there was an apparent conflict between the results of Elliott & Rose (1970, 1971) and Bennett *et al.* (1966), on the one hand and those of various authors who had obtained results at atmospheric pressure (e.g. Duffey & Porthouse 1972, Yamanouchi 1968, Yoshioka & Hasegawa 1970), on the other. This arose because the experiments done at elevated pressures indicated no effect of water flowrate while the results obtained at atmospheric pressure indicated a strong effect. It is now clear that the main reason for this difference is that in the atmospheric tests the water at the quench front was subcooled. The data obtained by the

Table 9. The best fit Biot number $(T_0 - T_s)$ and F_s obtained for three stainless steel, an inconel and a ziracaloy test section

Authors and test section	Pressure (bar)	Range of T_w (°C)	Number of points	Biot number	$T_0 - T_s$ (°C)	σ_{MIN} (°C)	F_s $\times 10^{-4}$
Elliott	3.43	225–468	38	166.8	38	8.5	5.42
& Rose	3.77	239–456	16	78.5	47	19.4	4.60
(1970)	7.87	240–466	58	999*	17	14.0	5.84
1st S.S.	21.7	272–479	53	131.6	50	8.3	6.59
[1]	52.8	322–442	34	88.0	56	9.3	6.15
Elliott	3.43	327–558	56	15.1	135	21.0	6.04
& Rose	7.87	322–545	49	31.1	99	23.8	6.24
(1970)	21.7	393–579	30	19.2	144	20.5	7.50
2nd S.S.	52.8	439–565	14	29.6	128	16.8	8.37
[1]							
Elliott	3.43	393–611	20	30.2	100	30.3	6.25
& Rose	7.87	341–612	20	999*	20	28.9	7.21
(1970)	21.7	341–576	68	59.8	76	20.1	6.72
Inconel	52.8	338–514	38	55.1	82	11.4	7.30
[3]							
Elliott	3.43	385–704	83	12.6	151	44.1	5.50
& Rose	7.87	400–713	75	999*	22	26.7	6.69
(1971)	21.7	383–717	80	999*	25	20.0	7.87
Zircaloy	52.8	369–613	60	999*	25	21.6	8.17
[4]							
Bennett	6.9	275–367	7	177.7	45	5.2	6.69
et al.	13.7	291–390	9	126.2	52	9.2	6.60
(1966)	20.7	287–439	36	201.0	46	6.6	7.41
S.S.	34.5	307–462	12	94.0	68	8.0	7.62
[1]	69.0	372–469	9	290.0	41	5.3	8.12

*No minimum σ obtained.

[ ] Refers to property set number in table 3.

Table 10. The best fit Biot number ($T_0 - T_q$), F_q and α obtained for atmospheric pressure rewetting results by various authors using subcooled water

Authors	Flow (g sec^{-1})	ΔT_q (°C)	Range of T_w (°C)	No. of points	Biot number	$T_0 - T_q$	σ_{MIN} (°C)	F_q $\times 10^{-4}$	α
Duffey	0.1	0	101–597	20	16.8	36.6	41.6	2.15	0.751
&	0.5	31	175–724	48	0.77	178.9	32.7	2.38	0.734
Porthouse	1.2	52	139–775	61	4.88	128.1	32.1	4.15	1.20
[1972)	6.2	73	175–778	56	5.04	176.3	27.8	5.88	1.50
inconel [3]	18.0	77	226–773	45	7.40	187.1	29.4	7.58	1.78
12 mm o.d.	27.0	77	273–725	57	368.0	49.5	30.4	13.18	3.00
0.85 mm wall	37.0	77	205–775	8	No minimum or plateau obtained				
Duffey	0.33	54	150–746	13	0.5*	182.6	52.3	3.97	0.748
et al.	0.92	66	205–750	12	0.5*	225.8	36.7	3.08	0.859
inconel [3]	2.1	73	202–750	13	1.96	192.3	25.4	5.29	1.39
6 mm o.d.	4.3	74	204–752	13	7.4	184.6	35.8	9.82	2.43
0.5 mm wall									
Shires (1964)									
et al.	5.0	80	112–346	4	80.0	43.9	7.5	5.30	1.40
S.S. [2]	10.0	80	177–343	6	44.0	66.4	30.6	6.02	1.50
15.9 mm o.d.	20.0	80	166–510	4	35.0	99.1	24.7	8.14	1.93
0.91 mm wall									
Yamanouchi									
(1968)	16.67	72	203–651	7	6.32	159.9	28.3	5.53	1.32
S.S. [2]	6.67	68	197–548	5	5.84	120.9	21.7	3.95	1.01
15 mm o.d.	1.67	38	201–499	4	1.01	204.3	73.2	2.92	0.833
1 mm wall									

The inlet water temperatures were ambient in all cases.
*No minimum σ obtained.
[ ] Refers to property set number in table 3.

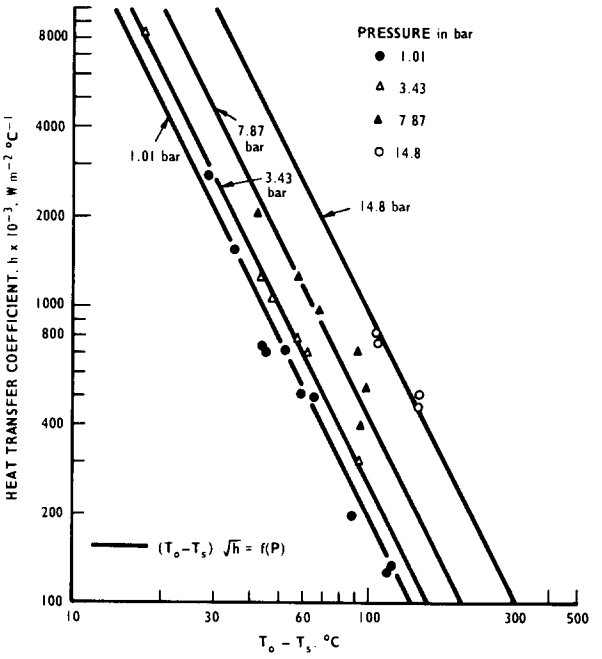

Fig. 11. Calculated heat-transfer coefficient vs $T_0 - T_s$ for the CERL falling film rig data obtained using saturated water.

present authors for the case of saturated water flows is illustrated in figure 12. This confirms the earlier results that there is no effect of flowrate (within the range considered) at high pressures but it does indicate a small effect of flowrate at pressures near atmospheric. This is represented by means of a correction factor k_G to the basic equation [10]. A suitable expression for k_G was

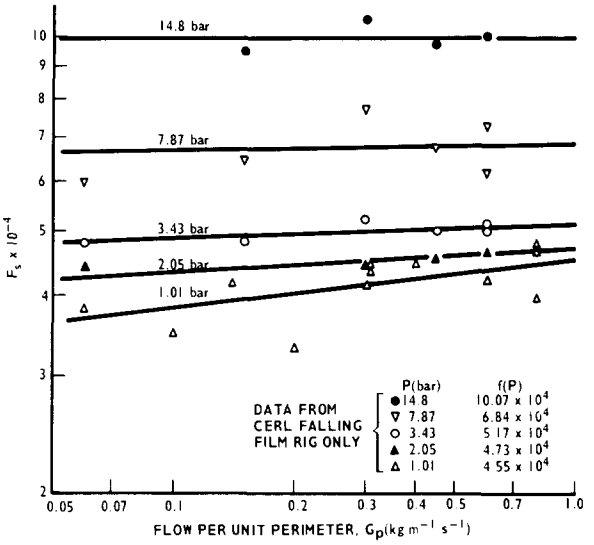

Figure 12. Plot of F_s vs G_p for various pressures compared to the equation $F_s = f(P)G_p^{0.076/P}$.

found to be

$$k_G = G_p^{0.0765/P} \qquad [11]$$

where G_p is the flow per unit perimeter (kg m^{-1} sec^{-1}). The complete correlation that gave the best description of all the results in Tables 5 and 9 was found to be

$$F_s = 4.52 \times 10^4 (1.0 + 1.216 \log_{10} P)^{1/2} G_p^{0.0765/P}. \qquad [12]$$

The average value of $T_0 - T_s$ indicated by both our own data in table 5 and the earlier data in Table 9 is very close to 67°C. Figure 13 shows a comparison between the correlation [12] and the experimental values of F_s obtained from all the available saturated falling film data. Most of the data lie within ±13% of the correlation. However our own results obtained at 14.8 bar are conspicuously high. The reason for this discrepancy is not known but it may be an effect of the tube wall thickness on the nucleate boiling heat-transfer process, since it is noted that the CERL test-section had a much thinner wall than previous test-sections examined at high pressures. Another suggestion (C. R. Thomas, private communication) is that the use of a mild steel vessel in the CERL facility causes fine oxide deposits on the heated rod which leads to enhanced nucleation at high pressures, where the nucleation superheat required is much reduced. Further tests are proposed, which should throw some light on this uncertainty.

5.2 *Falling films with subcooled water*

It is convenient to relate the data obtained with subcooled water at the quench front to that predicted for the corresponding situation with saturated quench water. For this purpose we define a parameter α by the equation

$$\alpha = \frac{F_q}{F_s(\text{calc.})} \qquad [13]$$

where F_s(calc.) is obtained from [12]. Figure 14 shows the data of tables 6 and 10 plotted in the form of α vs $G_p \Delta T_q$. As might be expected from the uncertainties in calculating ΔT_q and perhaps more particularly the fact that subcooled quench fronts tend to be non-uniform and unstable, it is seen that the scatter is fairly large but with most points lying within ±30% of a

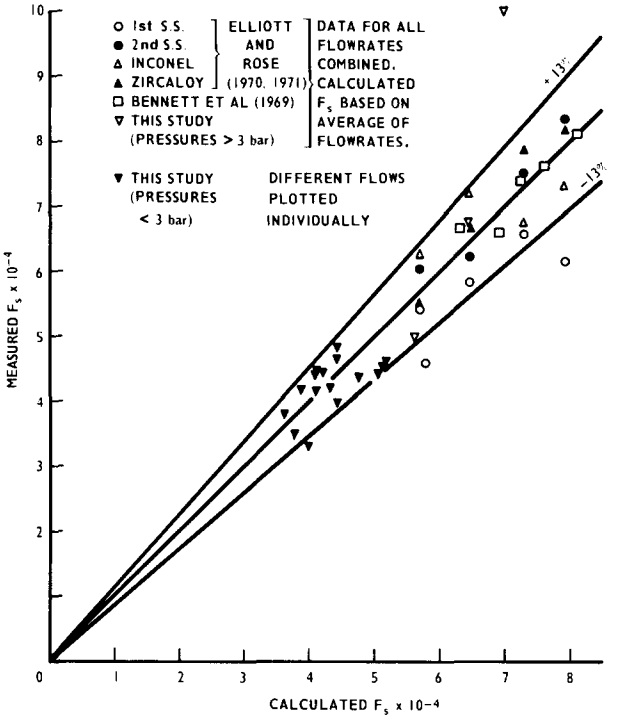

Figure 13. Comparison of available saturated falling film data with the equation

$$F_s = 4.52 \times 10^4 (1 + 1.216 \log_{10} P) G_p^{0.765/P}.$$

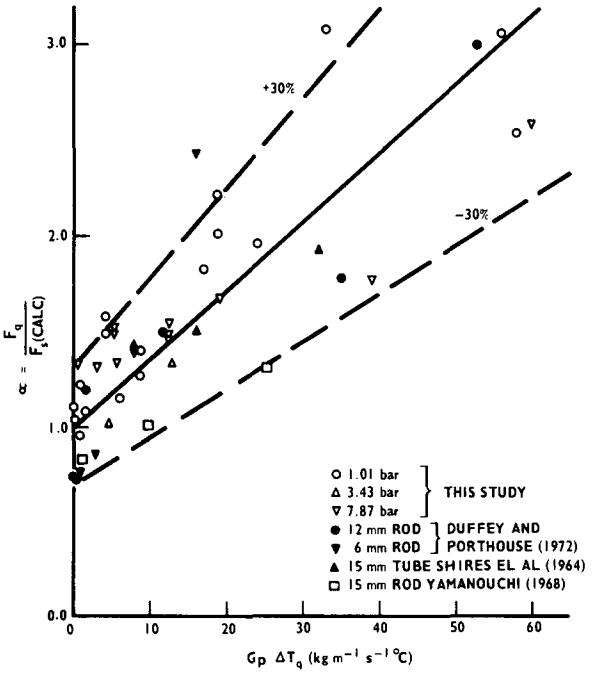

Figure 14. The parameter $\alpha = F_q/F_s$ (calc.) plotted vs $G_p \Delta T_q$ for falling film rewetting using subcooled water.

representative line. The suggested correlation for α is

$$\alpha = 1 + 0.036\Delta T_q G_p. \quad [14]$$

Again it is interesting to note that the average values for $T_0 - T_s$ $(= T_0 - T_q - \Delta T_q)$ obtained from our own data in table 6 and from previous data in table 10 are both approx. 78°C.

Taking [14] together with [13] and [12] we can propose a correlation for both saturated and subcooled quenching by falling films as follows:

$$F_q = 4.52 \times 10^4 (1 + 0.036\Delta T_q G_p)(1 + 1.216 \log_{10} P)^{1/2} G_p^{0.0765/P}. \quad [15]$$

5.3 *Bottom flooding with saturated water*

It was found that a direct comparison of the falling film and bottom flooding data on the basis of G_p was not possible—the values of F_s obtained from falling films on this basis were about twice those obtained from bottom flooding. This is not surprising since the important parameter must be the rate at which water is supplied to the quench front—not the rate at which it is supplied to the test vessel. An obvious parameter to choose would therefore be the flow velocity local to the quench front, but as a simplification it was decided to use the average coolant velocity. This ignores the effects of geometry and velocity profile on the boiling process.

For bottom flooding inside a tube the average velocity v (m sec^{-1}) is simply given by

$$v = \frac{4M}{\pi D^2 \rho} \quad [16]$$

where M is the mass flow rate (kg sec^{-1}), ρ is the liquid density (kg m^{-3}) and D is the tube bore (m).

In the case of falling films, the average velocity is given by

$$v = \frac{G_p}{\rho b} \quad [17]$$

where b is the film thickness (m).

Fulford (1964) carried out a review of correlations for film thickness calculations. He recommended that for laminar flow the Kapitza equation should be used, which together with [17] gives

$$v = \left[\frac{G_p^2 g}{2.4\rho\mu}\right]^{1/3} \quad \text{for} \quad \frac{G_p}{\mu} < 400 \quad [18]$$

where μ is the liquid viscosity (kg m^{-1} sec^{-1}).

In the turbulent regime, a correlation due to Brötz was recommended which together with [17] yields

$$v = \left[\frac{590 G_p g}{3\rho}\right]^{1/3} \quad \text{for} \quad \frac{G_p}{\mu} > 400. \quad [19]$$

At high saturation pressures the considerably lower viscosity of the liquid film causes it to be turbulent over a wider range of flowrates. The equations show that in this region, the velocity is only weakly dependent on the mass flow rate. This effect may go part of the way towards

explaining why in the falling film experiments the dependence of the rewetting velocity on G_p reduced as the saturation pressure was increased.

Figure 15 shows the data compared on the basis of the flow velocity and it may be seen that although the range of film velocities obtained in the falling film work is rather restricted, the data agree well. A best fit line to the data is given by

$$F_s = 4.24 \times 10^4 v^{0.15}. \qquad [20]$$

This very simple correlation provides a reasonable fit to all the saturated water data at atmospheric pressure and is close to the falling film correlation also shown in figure 15. Most of the points lie within ±30% of the correlation given by [20]. Figure 16 shows one set of experimental data, compared with curves generated using [20]. We note from table 7 that the average value of $T_0 - T_s$ (107°C) is somewhat higher than in the falling film experiments.

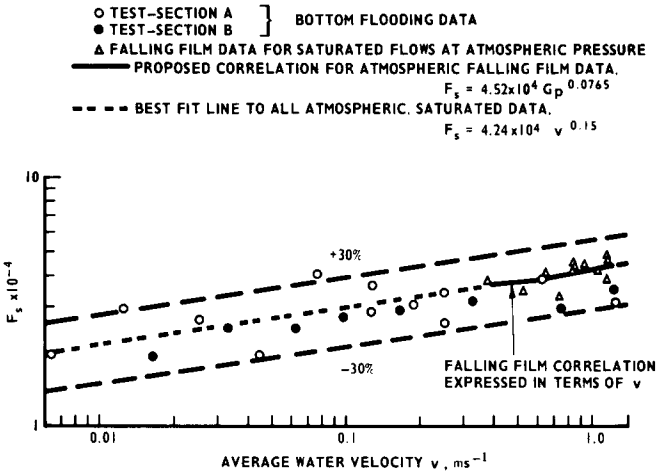

Figure 15. Comparison of values of F_s for falling film experiments with bottom flooding data based on average flow velocity.

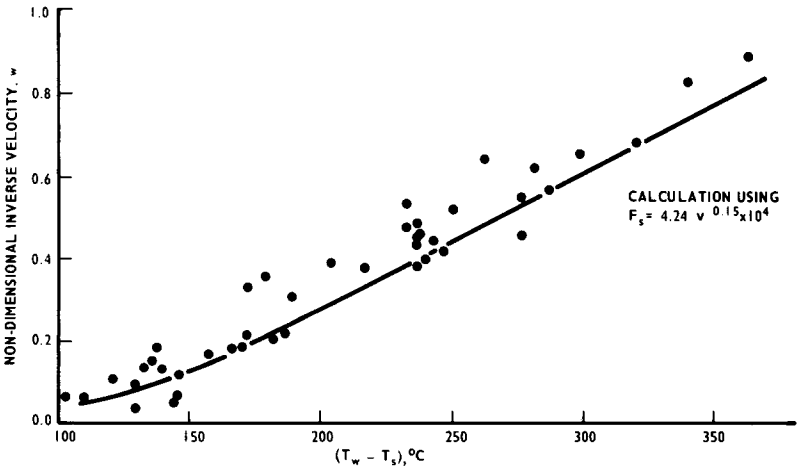

Figure 16. Comparison between saturated data for test section B at 20 g sec^{-1} and calculation using [16] and the REWET results from table (bottom flooding experiments).

5.4 *Bottom flooding with subcooled water*

Making the comparison on the basis of equal values of $v\Delta T_q$ the results in table 8 were examined to see whether there was a correspondence between the subcooled falling film and bottom flooding results similar to that found in the case of saturated water. However it was found

that the use of subcooled water in bottom flooding had a much greater effect than had been the case with the falling films.

Figure 17 shows the bottom flooding data plotted on the basis of $(1+v\Delta T_q^2)$. This parameter correlates the data well and two curves can be fitted to the points. However it is noted that there are systematic differences between test sections A and B for high values of $v\Delta T_q^2$. The two lines chosen are given by

$$\alpha = 0.4839(1+v\Delta T_q^2)^{0.346} \quad \text{for} \quad (1+v\Delta T_q^2) \geq 40, \tag{21}$$

$$\alpha = (1+v\Delta T_q^2)^{0.13} \quad \text{for} \quad (1+v\Delta T_q^2) \leq 40. \tag{22}$$

It is seen that most of the data lie within ±30% of these equations.

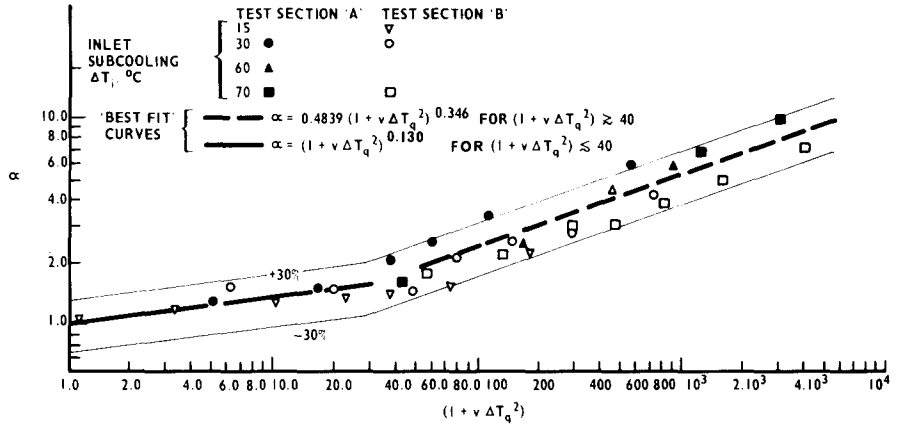

Figure 17. Bottom flooding data using subcooled water plotted as α against $v\Delta T_q^2$.

The average value of $T_0 - T_s$ $(= T_0 - T_q - \Delta T_q)$ given in Table 8 is 65°C. However it is noted that test-section B indicates an average of 112°C while test-section A indicates an average value of $(T_0 - T_s)$ which is actually negative (−5°C). There is no reason in principle why a negative value of $T_0 - T_s$ should not be obtained with subcooled rewetting, though it is not possible for $T_0 - T_q$ to become negative. The reason for this anomalous behaviour is not known, but in view of the large scatter on the data for subcooled flooding coupled with the basic insensitivity to the value of T_0 anyway, it is probably unwise to attach too much significance to this observation.

In view of the good agreement between bottom flooding and falling film rewetting for saturated flows it is at first sight surprising that there should be such a marked difference in behaviour when subcooled flows are used. A possible explanation for the difference could be that the large volume of subcooled water in the neighbourhood of the quench front in bottom flooding geometry is influencing the boiling process by condensing the vapour formed. With saturated flows this would not occur and it might be supposed that this volume of water plays little part in the local heat-transfer process during quenching. With subcooled falling films the boiling throws the film away from the surface and hence the subcooled water is only able to condense a limited volume of vapour.

6. USE OF THE CORRELATIONS FOR PREDICTION OF REWETTING RATES

Correlations have been suggested for the calculation of F_q for the cases of falling films and bottom flooding with both saturated and subcooled water. With a knowledge of the clad thickness ϵ and thermal conductivity k, the parameter $F_q\sqrt{(\epsilon/k)}$ may be calculated. This has dimensions of °C and is in effect a normalising temperature since when the wall temperature elevation $(T_w - T_q)$ is divided by this quantity the dimensionless parameter η is obtained as in [6]. Thus any error in F_q is equivalent to an error in the calculated wall temperature elevation.

The Biot number is obtained from the relation

$$Bi = \frac{F_q^2 \epsilon}{k(T_0 - T_q)^2}. \quad [23]$$

We have seen that $(T_0 - T_q)$ can vary over a substantial range, but also that provided $Bi \geq 5$, the rewetting rate is very insensitive to this parameter and the variation caused by the uncertainty in $(T_0 - T_q)$ is often much less than the experimental scatter. This is demonstrated further in figure 18, where the inconel and stainless steel data of Elliott & Rose (1970) obtained at 3.43 bar are compared with the suggested correlations for F_s taken together with extreme values for $T_0 - T_s$ of 20°C and 160°C. However a value for $T_0 - T_s$ must be chosen and it is therefore noted that the average values for each of Tables 5–10 range from 65°C up to 107°C, with an overall average value close to 80°C. Thus the authors recommend that the value for $T_0 - T_q$ should be given by

$$T_0 - T_q = \Delta T_q + 80 \ (°C) \quad [24]$$

for the cases of saturated or subcooled quenching by falling films or by bottom flooding.

With a knowledge of η and Bi, the corresponding value of w can of course be obtained from Table 1 or figure 2. Substitution of the material properties k, ϵ, ρ and c allows the rewetting velocity U to be obtained from [1].

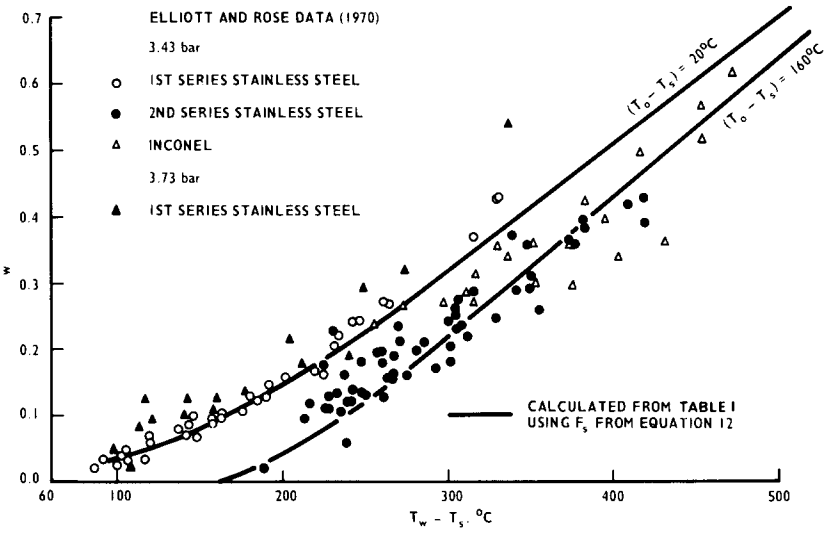

Figure 18. The comparison between the rewetting rate predicted from REWET results using F_s from [12] and the experimental data of Elliott & Rose (1970).

7. COMPARISON WITH THE DATA OF OTHER AUTHORS

The data of a number of authors have already been used in obtaining the falling film correlations given by [15], but those of Yoshioka & Hasegawa (1970) and Piggott & Porthouse (1975) were not amenable to the present form of analysis since they were obtained at too few wall temperatures. However these data can be used for comparison with the derived correlations. Figure 19 shows the correlation predictions compared with the atmospheric, falling film data of Yoshioka & Hasegawa (1970) assuming a value for $(T_0 - T_s)$ of 80°C. It is seen that the agreement is generally satisfactory, though the prediction of inverse wetting rate at $T_w = 500$°C, $T_i = 15$°C is a little too high. Figure 20 shows a comparison between the correlation of [15] and the data of Piggott & Porthouse (1975). Here the agreement with the data is good.

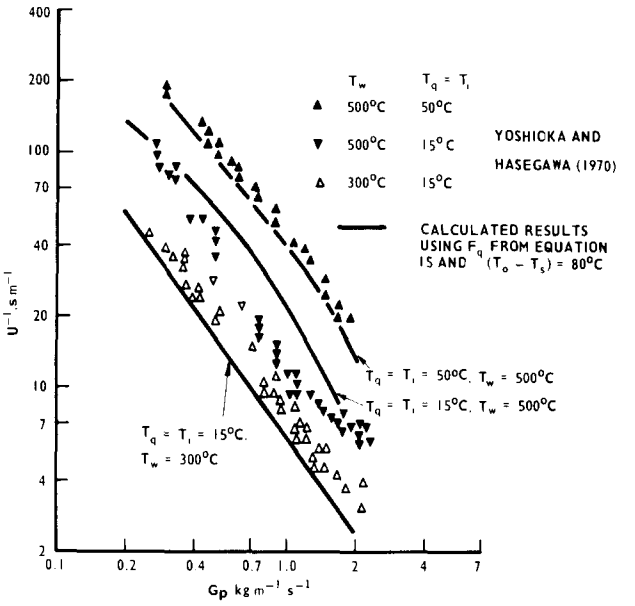

Figure 19. Comparison of falling film correlation with rewetting data of Yoshioka & Hasegawa (1970).

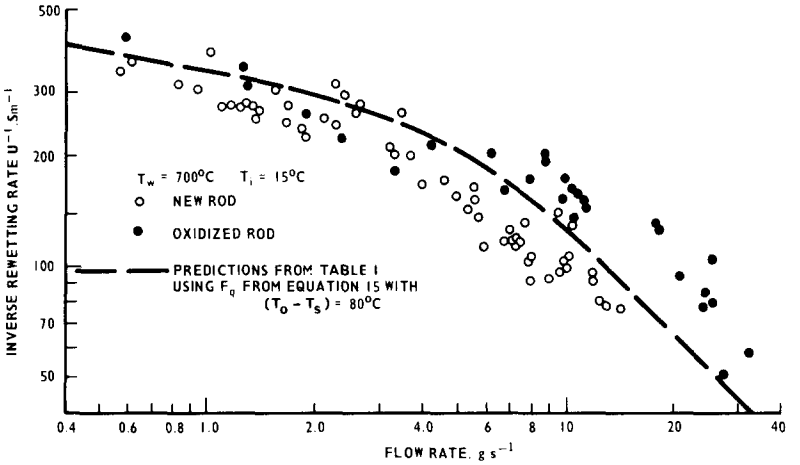

Figure 20. Comparison of predictions using [15] with the falling film data of Piggott & Porthouse (1975).

The bottom flooding correlations of [20–22] were compared with data for two other geometries, an annulus in which only the inner rod was heated (Piggott & Porthouse 1975), and a rod bundle (Thompson 1974). Figure 21 shows the comparison with the Piggott and Porthouse data and it may be seen that whilst at high subcoolings the correlations underestimate the effects of subcooling the trends are predicted and convergence towards the saturated water line is good. Quench front subcoolings were calculated using the methods given in the Appendix. Figure 22 shows comparisons with the Thompson data assuming (a) the quench temperature is unchanged from the inlet, and (b) the quench temperature is saturated. For the former case the agreement improves as flowrate increases, and for the latter case it improves as the flowrate decreases, and the two assumptions bracket the data. This behaviour is to be expected since the loss of subcooling from inlet to quench front increases with decreasing flow. From both the above comparisons there is good support for the saturated quench correlation (equation [20]), but only qualitative evidence for the subcooled quench correlations (equations [21 and 22]). It is reasonable to expect that if the subcooled water is condensing vapour near the quench front the effects could be geometry dependent, whereas with saturated water geometry would not be an important parameter.

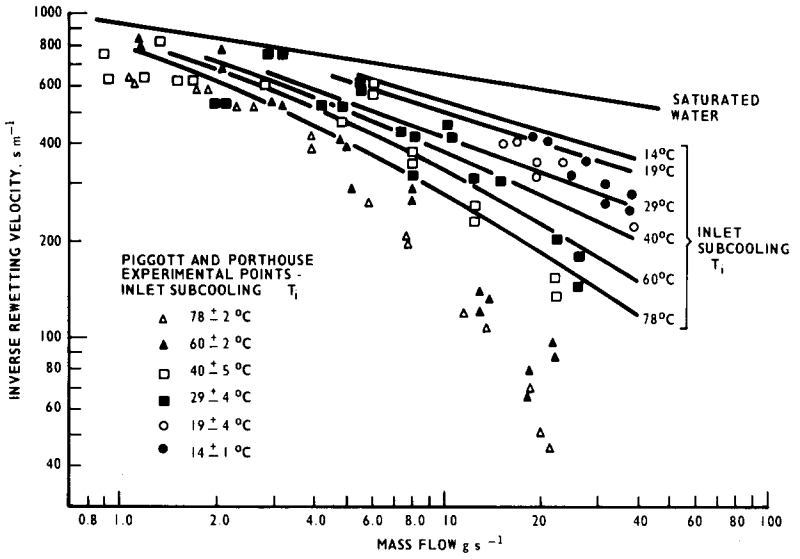

Figure 21. Piggott & Porthouse (1975) bottom flooding data for subcooled flows compared with the best fit curves from figures 15 and 17 [20, 21 and 22].

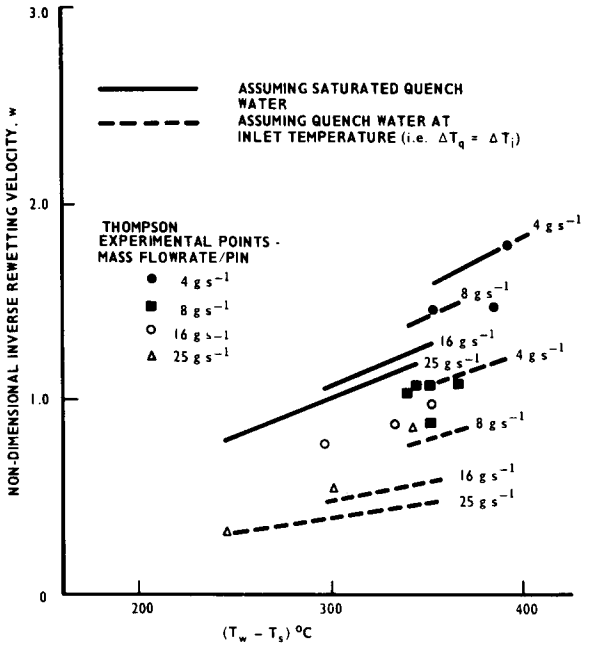

Figure 22. Thompson (1972) bottom flooding data for subcooled flows compared with the best fit curves from figures 15 and 17 [20, 21 and 22].

CONCLUSIONS AND DISCUSSION

The data analysed in this paper cover saturated and subcooled rewetting of falling films at pressures from atmospheric up to 69 bars, and a range of materials including stainless-steel, inconel and zircaloy. A fairly considerable amount of atmospheric bottom flooding data have also been analysed or compared with the derived correlations. In total, approx. 3750 data points have been used to derive the correlations and generally satisfactory comparisons have been made with a number of other results, which for one reason or another could not readily have been used to derive the correlations. The main conclusions are as follows.

(1) *Rewetting by falling films*

There is a strong dependence of rewetting velocity on the temperature of the water at the quench front. There is also a strong dependence on water flowrate when the water at the quench front is below its saturation temperature. The water temperature at the quench front is often different from the inlet water temperature due to a variety of heat-transfer mechanisms and this must be taken into account. The correlation

$$F_q = (T_0 - T_q)\sqrt{h} = 4.52 \times 10^4(1 + 0.036 G_p \Delta T_q)(1 + 1.216 \log_{10} P)^{1/2} G_p^{0.0765/P}$$

was found to provide a reasonable fit to the data which covered the range $1 < P < 69$ bar, $0.06 < G_p < 1.0$ kg m^{-1} sec^{-1} and $0 < \Delta T_q < 90$°C. The suggested value of $(T_0 - T_s)$ is 80°C though the results are insensitive to this value over a wide range.

(2) *Bottom flooding rewetting*

Rewetting rates using saturated water at atmospheric pressure agree well with saturated falling-film data when the water flow rates are related on the basis of average velocity in the film or the flooding flow.

A correlation which fits both the falling film and bottom flooding data obtained by the authors over the range $0.005 < v < 1.5$ m sec^{-1} is

$$F_s = 4.24 \times 10^4 v^{0.15}$$

using a value of 80°C for $(T_0 - T_s)$. Reported data for an annulus and a rod bundle suggest this correlation is not affected by geometry changes.

For bottom flooding using subcooled water the dependence of rewetting velocity on subcooling and flowrate is much stronger than with falling films, possibly due to vapour condensation at the quench front by the bulk liquid. Two correlations for the multiplier α which gave a reasonable fit to the atmospheric pressure data of the present work are

$$\alpha = 0.4839(1 + v\Delta T_q^2)^{0.346} \quad \text{for} \quad (1 + v\Delta T_q^2) \geqslant 40,$$

$$\alpha = (1 + v\Delta T_q^2)^{0.130} \quad \text{for} \quad (1 + v\Delta T_q^2) \leqslant 40.$$

Application of these correlations to data for an annulus and a rod bundle showed general agreement with the data trends, but indicated a need for further work on the effects of geometry.

(3) *Future research*

In spite of the fact that a large amount of data on rewetting have been successfully correlated, there are a number of outstanding questions in the general problem of calculating quench front velocities. There are several effects which have been identified but not yet quantified or understood.

Firstly there is the effect of a filler material such as UO_2 fuel on the rewetting velocity. It may be shown theoretically that at high rewetting velocities only a certain fraction of the cladding thickness has any influence on the process (Thompson 1973, Coney 1974). Clearly under these circumstances any filler material cannot have any effect either. However at slow rewetting rates (i.e. $w \gg 1$) this is no longer the case. Experimental evidence of this phenomenon is given by Piggott & Duffey (1975). However no theoretical work has yet been published in the open literature which allows this effect to be quantified.

Secondly, there is an effect of surface condition. This may be at least partly responsible for the considerable amount of scatter obtained in some experiments, though it is likely that

variations in the quench water temperature also play a part. Examples of the effects of surface condition have been described by Piggott & Porthouse (1975).

Thirdly, we note that although solutions have been obtained for the conduction process in rewetting, the mechanisms determining the actual values of h and T_0 are not understood. It seems likely that one of the reasons why high values of h are observed is that the high heat-flux area is confined to such a narrow region (~1 mm). If a tube wall is chosen which has a significantly different thickness, the width of this region changes and we cannot say whether the values of h and T_0 will be affected. The experimental evidence given here indicates that this could be occurring at high pressures, though the effect could be attributed to the presence of an oxide layer.

Finally, further experimental results and analysis are required for the case of bottom flooding particularly at elevated pressures. In these experiments it is important for the analysis of the quench front behaviour that both the wall temperature just prior to quenching and the water temperature at the quench front should be determined.

(4) *Use of the correlations*

Application of the correlations in circumstances outside the range of experimental conditions used in their derivation should be regarded as speculative.

Acknowledgements—The authors are grateful to the Technical Services personnel at CERL who provided the high pressure rewetting facility. The work was done at the Central Electricity Research Laboratories and is published by permission of the Central Electricity Generating Board.

REFERENCES

BENNETT, A. W., HEWITT, G. F., KEARSEY, H. A. & KEEYS, R. K. F. 1966 The wetting of hot surfaces by water in a steam environment at high pressure. AERE-R5746.

BUTTERWORTH, D. & OWEN, R. G. 1975 RS 133: The quenching of hot surfaces by top and bottom flooding—a review. AERE-R 7992.

CHUN, K. R. & SEBAN, R. A. 1971 Heat transfer to evaporating liquid films. *Trans. Am. Soc. Mech. Engrs, J. Heat Transfer* **93**, 391–396.

CONEY, M. W. E. 1974 Calculation of the rewetting of hot surfaces. *Nucl. Engng Design* **31**, 246–259.

DUFFEY, R. B. & PORTHOUSE, D. T. C. 1972 Experiments on the cooling of high temperature surfaces by water jets and drops. Proc. of the CREST specialist meeting on emergency core cooling for light water reactors. Technische Universität Munchen, 18–20 October.

ELLIOTT, D. F. & ROSE, P. W. 1970 The quenching of a heated surface by a film of water in a steam environment at pressures up to 53 bar. AEEW-M976.

ELLIOTT, D. F. & ROSE, P. W. 1971 The quenching of a heated zircaloy surface by a film of water in a steam environment at pressures up to 53 bar. AEEW-M1027.

FULFORD, G. D. 1964 *The Flow of Liquids in Thin Films*, Advances in Chemical Engineering, Vol. 5. Academic Press, New York.

HSU, S. T. 1963 *Engineering Heat Transfer.* Van Nostrand, New York.

PIGGOTT, B. D. G. & DUFFEY, R. B. 1975 Quenching of irradiated fuel pins. *Nucl. Engng Design* **32**, 182–190.

PIGGOTT, B. D. G. & PORTHOUSE, D. T. C. 1975 A correlation of rewetting data. *Nucl. Engng Design* **32**, 171–181.

SEMERIA, R. & MARTINET, B. 1965 Calefaction spots on a heated wall: temperature distribution and resorption. *Proc. Instn Mech. Engrs* **130**, 192–205.

SHIRES, G. L., PICKERING, A. R. & BLACKER, P. T. 1964 Film cooling of vertical fuel rods. AEEW-R343.

THOMPSON, T. S. 1972 An analysis of the wet-side heat transfer coefficient during rewetting of a hot dry patch. *Nucl. Engng Design* **22**, 212–234.

THOMPSON, T. S. 1973 On the process of rewetting a hot surface by a falling liquid film. AECL-4516.

THOMPSON, T. S. 1974 Rewetting of a hot surface. *5th Int. Heat Transfer Conf.*, Tokyo.

WAYNER, P. C., KAO, Y. K. & LA CROIX, L. V. 1976 The interline heat transfer coefficient of an evaporating wetting film. *Int. J. Heat Mass Transfer* **19**, 487–492.

YAMANOUCHI, A. 1968 Effect of core spray cooling in transient state after loss of coolant accident. *J. Nucl. Sci. Tech.* **5**, 547–558.

YOSHIOKA, K. & HAWEGAWA, S. 1970 A correlation in displacement velocity of liquid film boundary formed on a heated surface in emergency cooling. *J. Nucl. Sci. Tech.* **7**, 418–425.

APPENDIX
THE CALCULATION OF QUENCH FRONT TEMPERATURE FOR WATER FLOWS SUBCOOLED AT INLET

The assumption is made that there is no temperature gradient in the water in the direction normal to the direction of flow. This is a reasonable approach for thin falling films, but may not be realistic for bottom flooding geometries where there could be considerable temperature variation across the flow.

Consider an element of water of axial length dz travelling along the cladding. We have the following thermal processes.

(a) The heat $dH(J)$ taken up by the element in going from inlet to quench front is

$$dH = M\frac{dz}{v}C_p(T_q - T_i) \qquad [A3.1]$$

where v is the water velocity ($m\,sec^{-1}$) and M the mass flow rate ($kg\,sec^{-1}$) and C_p is the specific heat of water ($J\,kg^{-1}\,°C^{-1}$).

(b) The heat released from electrical heating of the test section to the water element is $dQ_1(J)$ where

$$dQ_1 = P_i L\frac{dz}{v} \qquad [A3.2]$$

where P_i is the electrical power per unit length ($W\,m^{-1}$) and L is the distance between the inlet and the quench front (m).

(c) In the quenching process heat is given up by the clad, which cools from T_w to T_q. Further heat is extracted upstream of the quench front to cool the clad from T_q down to T_i at the water inlet. This latter heat is given by:

$$dQ_2 = \rho c \epsilon \pi D(T_q - T_i)U\frac{dz}{v}. \qquad [A3.3]$$

(d) Heat is released to the water in falling film geometry by steam from the environment condensing into the film. This is given by

$$dQ_3 = \bar{h}dz\left[T_s - \frac{(T_q + T_i)}{2}\right]\pi DL \qquad [A3.4]$$

where $\bar{h}$ is the condensation heat-transfer coefficient ($W\,m^{-2}\,°C^{-1}$). Values for this were

obtained from a correlation given by Chun & Seban (1971), There is an increase of film mass flow resulting from this condensation, but for cases analysed so far this has been very small.

(e) The fill of the heater rod, or the fuel in a fuel pin loses heat to the coolant over a long time period. The problem may be analysed as a transient conduction problem for a cylinder subjected to a sudden surface temperature change. This approach assumes axial conduction in the filler material can be ignored for the purpose of calculation of T_q. It also assumes that there is good surface heat-transfer such that the heat loss is controlled by internal conduction. Charts of the solution were produced by Groeber (Hsu 1963), expressing $\beta(t)$ the fractional heat loss from the clad in time t, as a function of the surface heat-transfer and the thermal conduction in the rod. The total amount of heat released from the fill to the water element dz can be simplified to

$$dQ_4 = \frac{dz}{v} \rho_i c_i \frac{\pi d_i^2}{4} (T'_w - T_i) U \beta \frac{L}{U}. \qquad [A3.5]$$

$\beta(L/U)$ is found from the charts for a time period L/U, the time taken for the quench front to travel the distance L. T'_w is the initial fill temperature. This will be given approximately by T_w for a fill inside a tube heated slowly by passing current down the tube. For an internal heating element and a reactor fuel pin it may be necessary to calculate the initial radial temperature distribution.

From a heat balance

$$dH = dQ_1 + dQ_2 + dQ_3 + dQ_4. \qquad [A3.6]$$

In any given experiment some of the terms dQ_1 to dQ_4 will generally be zero. It may be seen that the further the quench front proceeds the lower will be the subcooling and it is thus important to know the exact geometry of an experiment before the loss of subcooling can be assessed.